Supporting Information

Vanadium defect-engineering in molybdenum disulfide for electrochemical nitrate reduction

*Miao Yu [a, 1], Hao Huang [b, 1], Jie Hu [a], Shuang Wang [a, c, *], Jinping Li [c, *], Dingsheng Wang [d, *]*

a. College of Environmental Science and Engineering, Taiyuan University of Technology, Jinzhong 030600, Shanxi, P. R. China. E-mail: wangshuang@tyut.edu.cn

b. Department of Microsystems, University of South-Eastern Norway, Borre 3184, Norway

c. Shanxi Key Laboratory of Gas Energy Efficient and Clean Utilization, Taiyuan University of Technology, Taiyuan 030024, Shanxi, P. R. China. E-mail: jpli211@hotmail.com

d. Department of Chemistry, Tsinghua University, Beijing 100084, China. E-mail: wangdingsheng@mail.tsinghua.edu.cn

‡ These authors contribute equally to this work.

1. Chemicals and materials

Sodium sulfate anhydrous (Na_2SO_4, ACS, ≥99.0%), Ammonium chloride(NH_4Cl, Cell culture specific), Sulfanilamide ($C_6H_8N_2O_2S$, AR, ≥99%), N-(1-naphthyl) ethylenediamine dihydrochloride ($C_{12}H_{14}N_2 \cdot 2HCl$, ACS, >98%), Phosphoric acid (H_3PO_4, ACS, ≥85 wt. % in H_2O), Salicylic acid ($C_7H_6O_3$, ACS, ≥99.0%), Sodium citrate ($C_6H_5Na_3O_7$, 98.0%), Sodium hypochlorite solution (NaClO, AR, 6-14%), Sodium nitroferricyanide dehydrate ($C_5FeN_6Na_2O.2H_2O$, 99.98% metals basis), Ammonium chloride-15N ($^{15}NH_4Cl$, abundance: 99 atom%, ≥98%), Sodium nitrate -15N ($^{15}NaNO_3$, abundance: 99atom%, ≥98.5%), Sodium hydroxide (NaOH, Ph. Eur., BP, NF, E524, 98-100.5%), Potassium chloride (KCl, GR, 99.8%), Thioacetamide (C_2H_5NS, ACS, 99.0%), Sodium molybdenum oxide, anhydrous ($MoNa_2O_4$, 99%), Maleic acid ($C_4H_4O_4$,AR, ≥99.0%), Deuterium oxide(D_2O, 99.9 atom % D) are all purchased from Aladdin Chemical reagent Co., Ltd. (Shanghai, China) without further purification. Sodium orthovanadate (Na_3VO_4, AR), Ethanol absolute (C_2H_6O, AR, ≥99.7%), Sodium nitrate ($NaNO_3$, AR, ≥99.0%), Sodium nitrite ($NaNO_2$, AR, ≥99%), L-Cysteine ($C_3H_7NO_2S$, BR, ≥98.5%), Sulfuric acid (H_2SO_4, GR, 95.0～98.0%), Hydrochloric acid (HCl, AR, 36.0～38.0%), hexadecyl trimethyl ammonium bromide ($C_{19}H_{42}BrN$, TBA, > 99%) are purchased from Sinopharm Chemical Reagent Co., Ltd. Nafion (5 wt.%) solution was purchased from Sigma-Aldrich Chemical Reagent Co., Ltd. The ultrapure water used throughout all experiments was purified through a Millipore system. The high-purity argon gases used in the experiment came from Anxuhongyun technology

development co. LTD. All reagents were analytical reagent grade without further purification.

2. Synthesis of MoS_2

The synthesis method is derived from literature[1]. Briefly, 3 mmol sodium molybdate ($MoNa_2O_4$) and 3 mmol L-cysteine ($C_3H_7NO_2S$) were separately dissolved into 30 mL deionized water. The two solutions were mixed under stirring for 20 min and were subsequently transferred to a Teflon-lined, 100-mL autoclave reaction vessel. After hydrothermal treatment at 200 °C for 24 h, the reaction vessel was naturally cooled down to room temperature. The resultant black precipitates were collected by filtration, washed with deionized water and ethanol, and dried under vacuum at 60 °C for 3 h.

3. Preparation of the V-MoS_2/CP Electrode

Typically, 4 mg of V-MoS2 powder and 20 μL of Nafion solution (5 wt %) were scattered in a mixture of 1mL ultra-pure water and 1mL anhydrous alcohol by ultrasonic treatment for 1h (50 HZ) to form a homogeneous liquid. Then, 500 μL of the dispersion was evenly loaded on a CP with an area of 1×1 cm^2 and dried under a baking lamp for 1 h at room temperature. The loading amount of V-MoS_2 was approximately 1mg.

4. Nafion 117 pre-treatment

The Nafion 117 membrane was boiled in 3% H_2O_2 solution for 30 min to remove organic impurities. The membrane surface of Nafion 117 was repeatedly cleaned with deionized water, and then boiled in 0.5 M H_2SO_4 solution for 1 h. The Nafion membrane is stored in deionized water for later use. After each electrochemical

reaction, the membrane was placed in deionized water for 30 seconds each time for 3 times to remove residual impurities and contaminants on the surface to avoid affecting the results of the next experiment.

5. Ion concentration detection methods

The UV-Vis spectrophotometer was used to detect the ion concentration of pre- and post-test electrolytes after dilution to appropriate concentration to match the range of calibration curves. Three parallel samples were prepared simultaneously for all electrolyte samples during measurement. The specific detection methods are as follow:

Detection of ammonia. The indophenol blue method with modification was used for spectrophotometrically measuring the concentration of produced NH_3. In particular, 1mL electrolyte was transferred from the electrolytic cell into a 10 mL sample bottle and diluted to 2mL. Subsequently, 1 M NaOH solution (2 mL) containing 5 wt% sodium citrate and 5 wt% salicylic acid was added to the aforementioned solution, followed by addition of 0.05 M NaClO (1 mL) and 0.2mL of 1 wt.% $C_5FeN_6Na_2O$ (sodium nitroferricyanide). After cover the sample bottle and mixing the above solution well, the compound was standed for 2 h under room temperature and the UV-Vis absorption spectrum was detected at a wavelength of 655 nm. The concentration absorbance curve was made by a series of standard ammonium chloride solutions.

Detection of nitrate-N. Firstly, 200 μL electrolyte was taken out from the electrolytic cell and diluted to 5 mL to measurement range in a 10 mL sample bottle. Then, 100 μL 1 M HCl and 10μL 0.8 wt% H_2SO_4 solution were added into the aforementioned

solution. After 15 minutes, the absorbance was detected by UV-Vis spectrophotometry at a wavelength of 220 nm and 275 nm. The final absorbance of nitrate-N was confirmed based on the following formula:

$$A = A_{220nm} - 2A_{275nm} \ (1)$$

The calibration curve can be obtained through different concentrations of $NaNO_3$ solutions and the corresponding absorbance.

Determination of nitrite. Nitrite chromogenic agent is sensitive and should be stored properly after configuration. Color developer configuration process: 100mg of N-(1-naphthyl) ethylenediamine dihydrochloride, 2g of p-aminobenzenesulfonamide, and 5 mL of phosphoric acid (ρ=1.685 g mL^{-1}) were added into 25 mL of deionized water and mixed thoroughly as the color reagent. The electrolytes were diluted 5 times, 5 mL of diluted electrolyte and 0.1 mL of color reagent were mixed together in a 10 mL bottle. Waiting for 20 min at room temperature, the absorbance was tested by UV-Vis spectrophotometry at a wavelength of 540 nm. The calibration curve can be obtained through different concentrations of $NaNO_2$ solutions and the corresponding absorbance.

6. Calculation of the conversion, yield, and selectivity.

The conversion of NO_3^- was calculated following the equation:

$$NO_3^- - \text{ conversion (nitrate removal rate)} = \frac{\Delta C_{NO_3^-}}{C_0} \times 100\% \ (2)$$

The yield of NH_4^+(aq) was calculated following the equation:

$$\text{Yield } NH_4^+ = (C_{NH_4^+} \times V)/(M_{NH_4^+} \times t \times m) \ (3)$$

The selectivity of the products calculated following the equations:

$$NH_4^+ \text{ selectivity } \left(S_{NH_4^+}\right) = \frac{\Delta C_{NH_4^+}}{\Delta C_{NO_3^-}} \times 100\% \ (4)$$

$$NO_2^- \text{ selectivity } \left(S_{NO_2^-}\right) = \frac{\Delta C_{NO_2^-}}{\Delta C_{NO_3^-}} \times 100\% \ (5)$$

Where $C_{NH_4^+}$ is the concentration of NH_4^+ (aq), $C_{NO_2^-}$ is the concentration of NO_2^- (aq), $\Delta C_{NO_3^-}$ is the concentration difference of NO_3^- before and after electrolysis, C_0 is the initial concentration of NO_3^-, V is the electrolyte volume, t is the electrolysis time, m is the mass of catalyst.

7. 15N Isotope Labeling Experiments

The isotopic labeling nitrate reduction experiments which were used $Na_{15}NO_3$ (99 atom% ^{15}N) as the providing N-source was carried out to clarify the source of ammonia. 0.5 M Na_2SO_4 was acted as electrolyte and $Na_{15}NO_3$ with a concentration of 100ppm $15NO_3^-$-15N was added into the cathode compartment as the reactant. After NITRR reaction, electrolyte with obtained $15NH_4^+$-15N was moved out and the pH value was adjusted to be weak acid (pH≈2) with 4M H_2SO_4 for further quantification by 1H NMR (600MHz) with external standards of maleic acid ($C_4H_4O_4$, 100ppm). The calibration curve was prepared as follows: First, a series of $15NH_4^+$-15N solutions ($(15NH_4)_2SO_4$)) with known concentration (10, 20, 40, 60, 80 ,100ppm) were prepared in 0.5 M Na_2SO_4 as standards; Second, 50mL of the $15NH_4^+$-15N standard solution with different concentration was mixed with 5mg maleic acid; Third, 50 μL deuterium oxide (D_2O) was added in 0.5 mL above mixed solution for the NMR detection; Fourth, the calibration was achieved using the peak area ratio between $15NH_4^+$-15N and maleic acid because the $15NH_4^+$-15N concentration and the area ratio were positively correlated. Due to the peak area of NMR is directly related to the content of ammonium, the concentration of NH_4^+-N can be quantitatively determined by 1H NMR with external standards (maleic acid). The proton signal of maleic acid appears at δ = 6.30-6.40 ppm. The 1H NMR spectra of $15NH_4^+$ show double peaks at δ = 7.11 and 6.99 ppm, while $14NH_4^+$ show triple peaks at δ = 7.15, 7.06 and 6.97 ppm.

8. DFT Calculations

DFT simulation of V-MoS_2 and MoS_2 slabs were calculated by using a generalized gradient approximation (GGA) of exchange-correlation functional in the Perdew, Burke, and Ernzerhof (PBE). To avoid periodic interaction, a vacuum layer of 30 Å was established for the slabs. Meantime, PDOS calculation was performed by GGA+U functional for 3d-orbit. A plane-wave energy cut off of 500 eV was used together with normconserving pseudopotentials, and the Brillouin zone was sampled with a 2 × 2 × 1 Monkhorst-Pack grid. The structure was fully optimized until the force on each atom was less than 10^{-3} eV $Å^{-1}$. On the other side, the free energy (ΔG) was computed from

$$\Delta G = \Delta E + \Delta ZPE - T\Delta S \quad (6)$$

where *ΔE* means the total energy, *ΔZPE* was the zero-point energy, the entropy (*ΔS*) of each adsorbed state were obtained from DFT calculation, whereas the thermodynamic corrections for gas molecules were from standard tables.

Table S1. Compositions of the V-doped MoS_2 nanosheets prepared with reactants of various vanadium contents.

Samples	Reactants			
	Na_3VO_4 (mmol)	Na_2MoO_4 (mmol)	C_2H_5NS (mmol)	V/(V+Mo) ratio
5%V-MoS_2	0.1	1.9	8	5%
10%V-MoS_2	0.2	1.8	8	10%
15%V-MoS_2	0.3	1.7	8	15%
20%V-MoS_2	0.4	1.6	8	20%
25%V-MoS_2	0.5	1.5	8	25%
30%V-MoS_2	0.6	1.4	8	30%

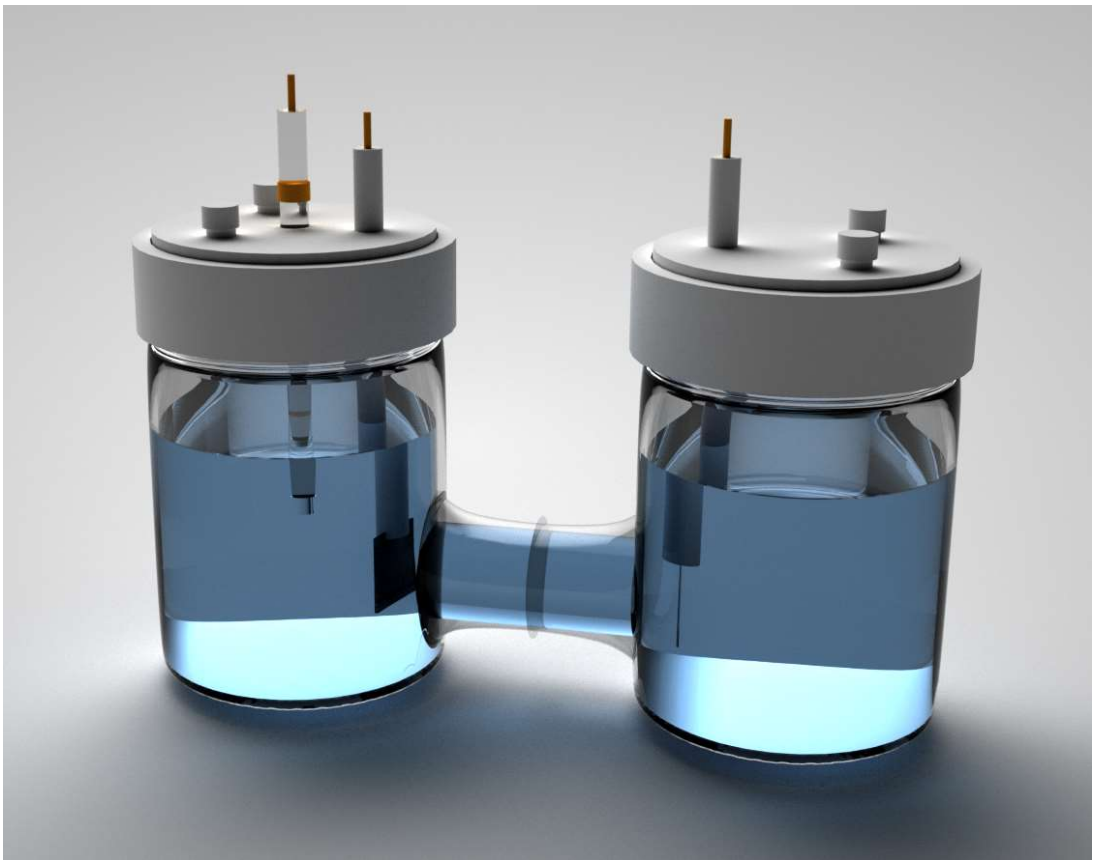

Fig. S1. Nitrate electrocatalytic reduction reactor.

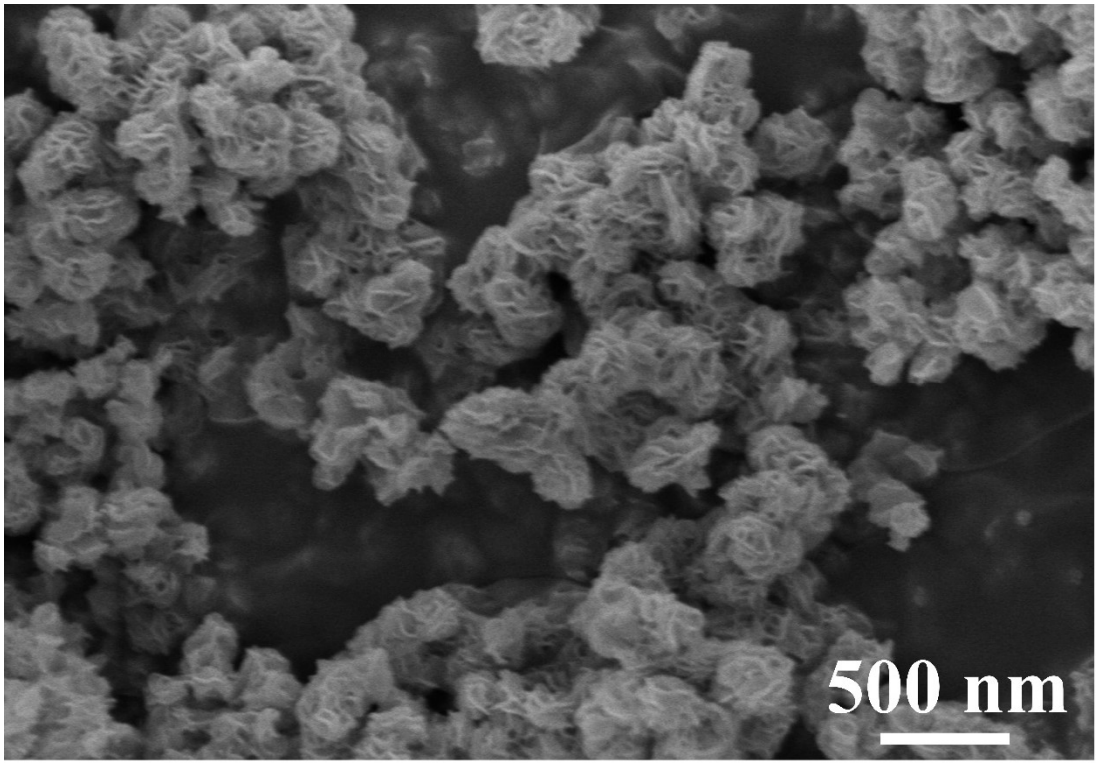

Fig. S2. SEM image of pure MoS_2.

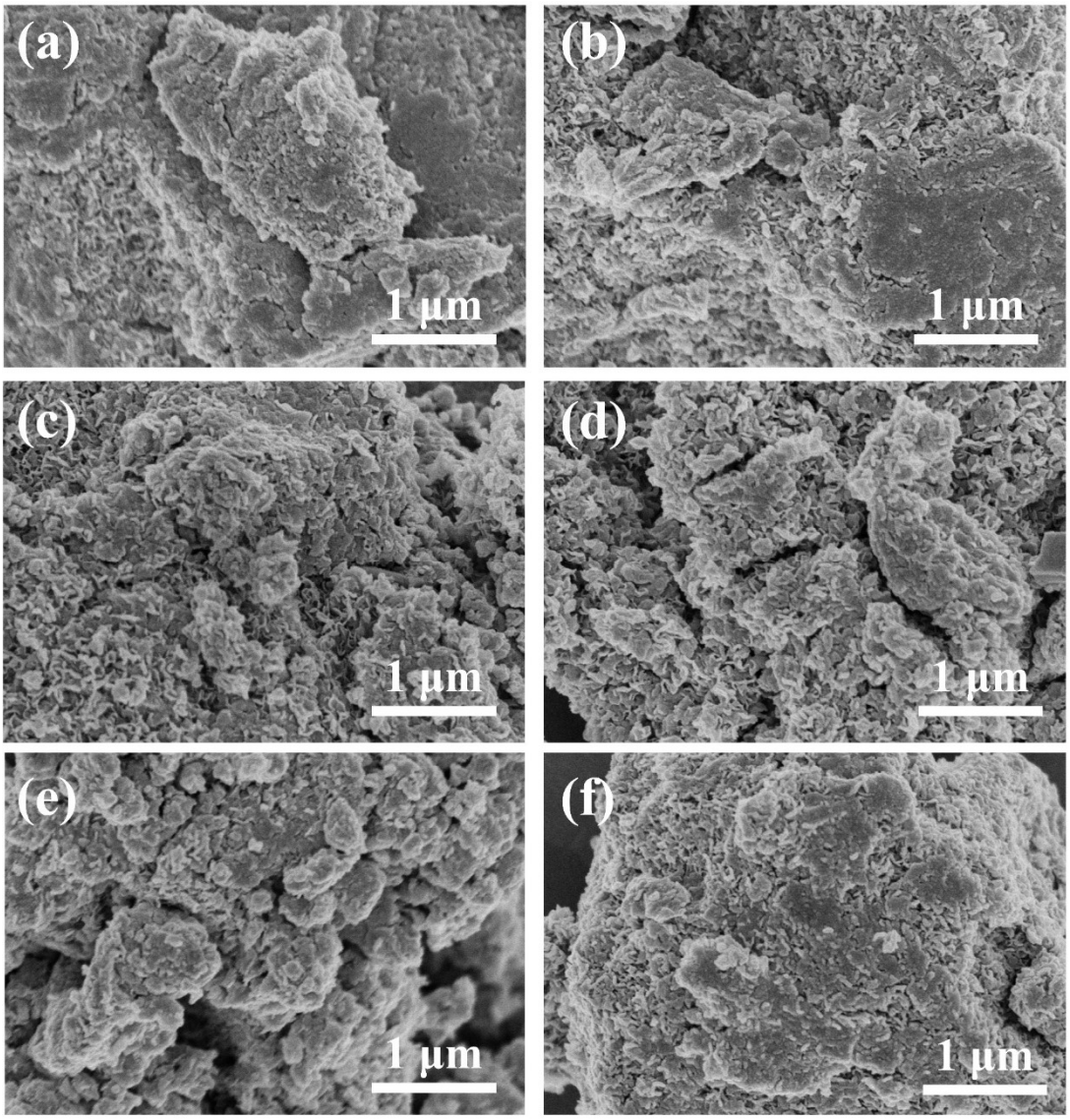

Fig. S3. SEM images. (a) 5%V-MoS_2. (b) 10%V-MoS_2. (c) 15%V-MoS_2. (d) 20%V-MoS_2. (e) 25%V-MoS_2. (f) 30%V-MoS_2.

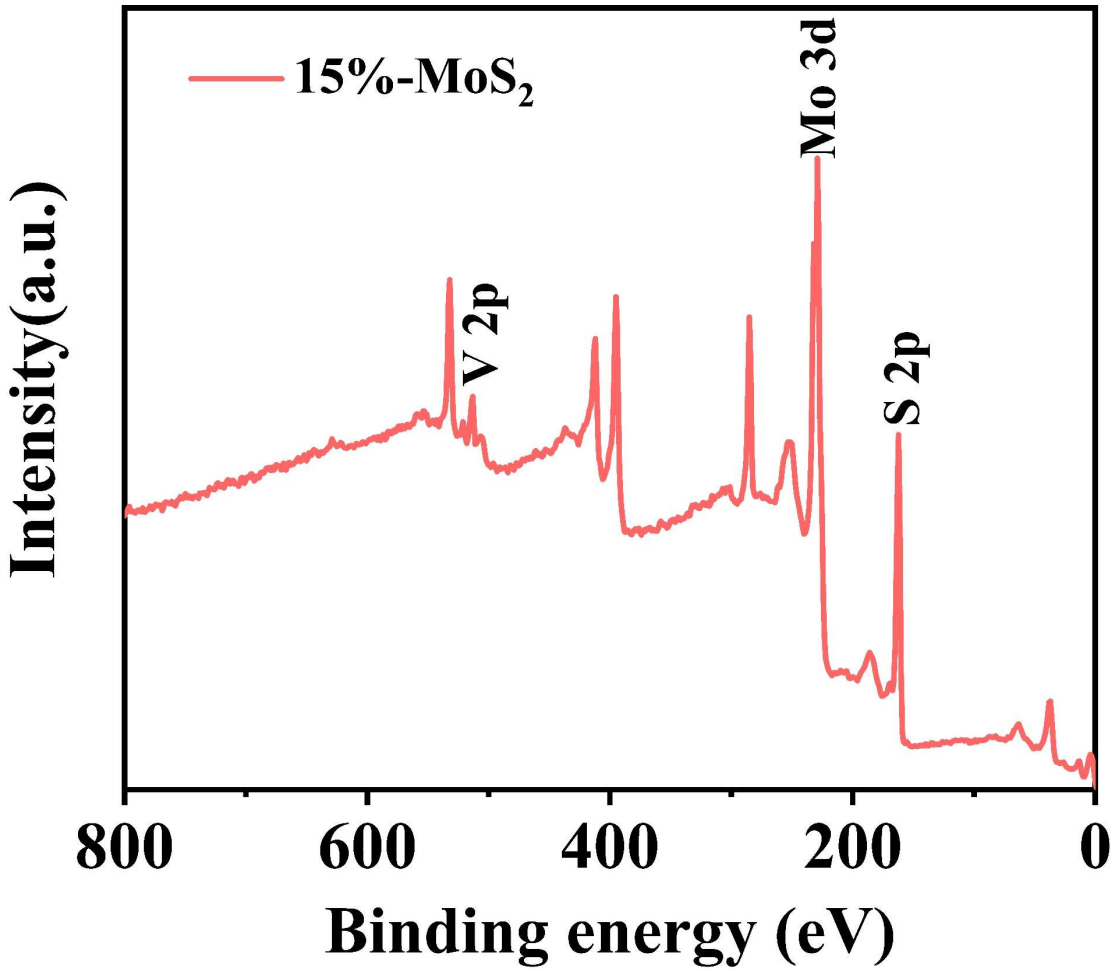

Fig. S4. Wide-scan survey XPS spectra of 15%V-MoS_2.

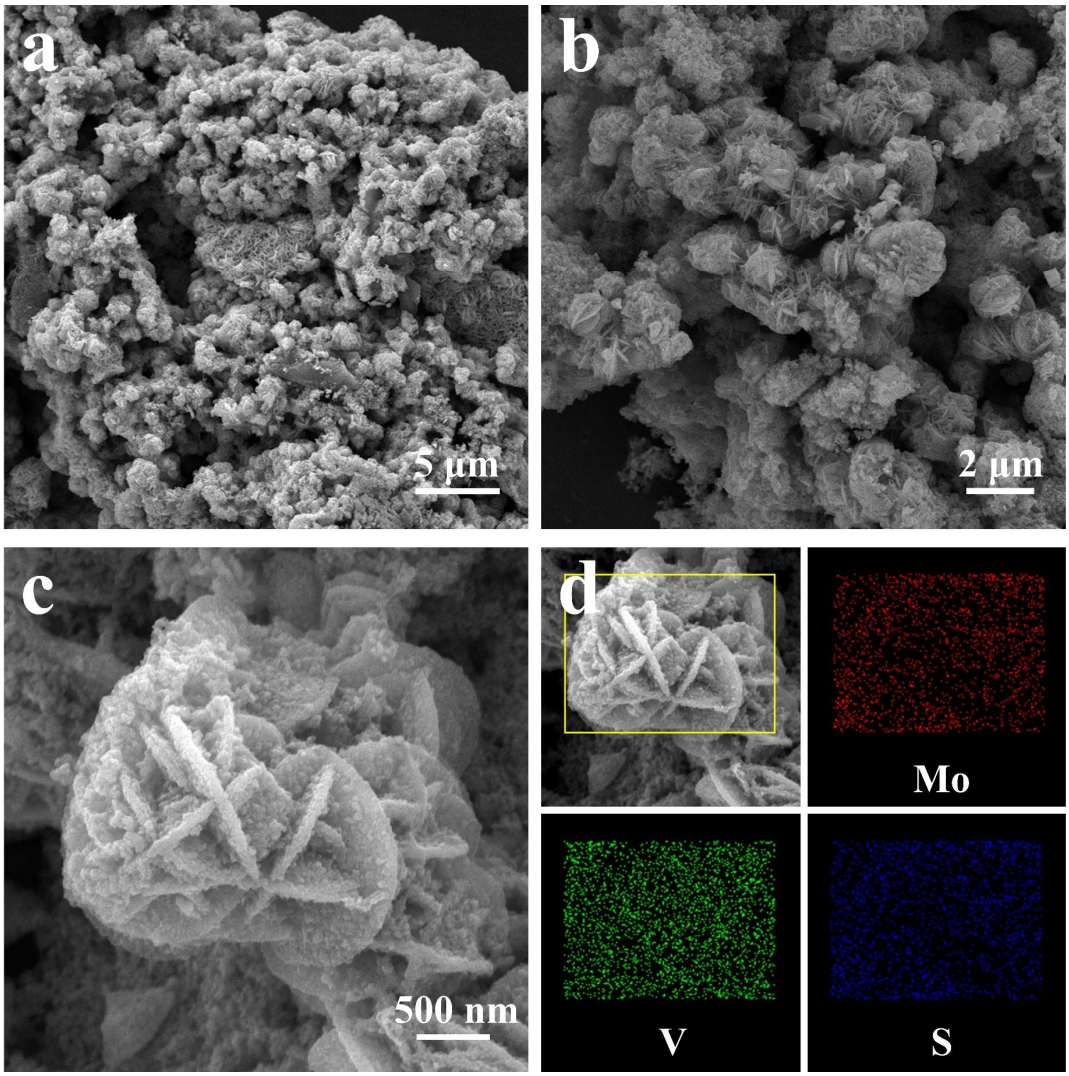

Fig. S5. (a, b) SEM images and (c, d) corresponding elemental mappings for the marked region of the 15%V-MoS_2 electrocatalyst after electrochemical NITRR.

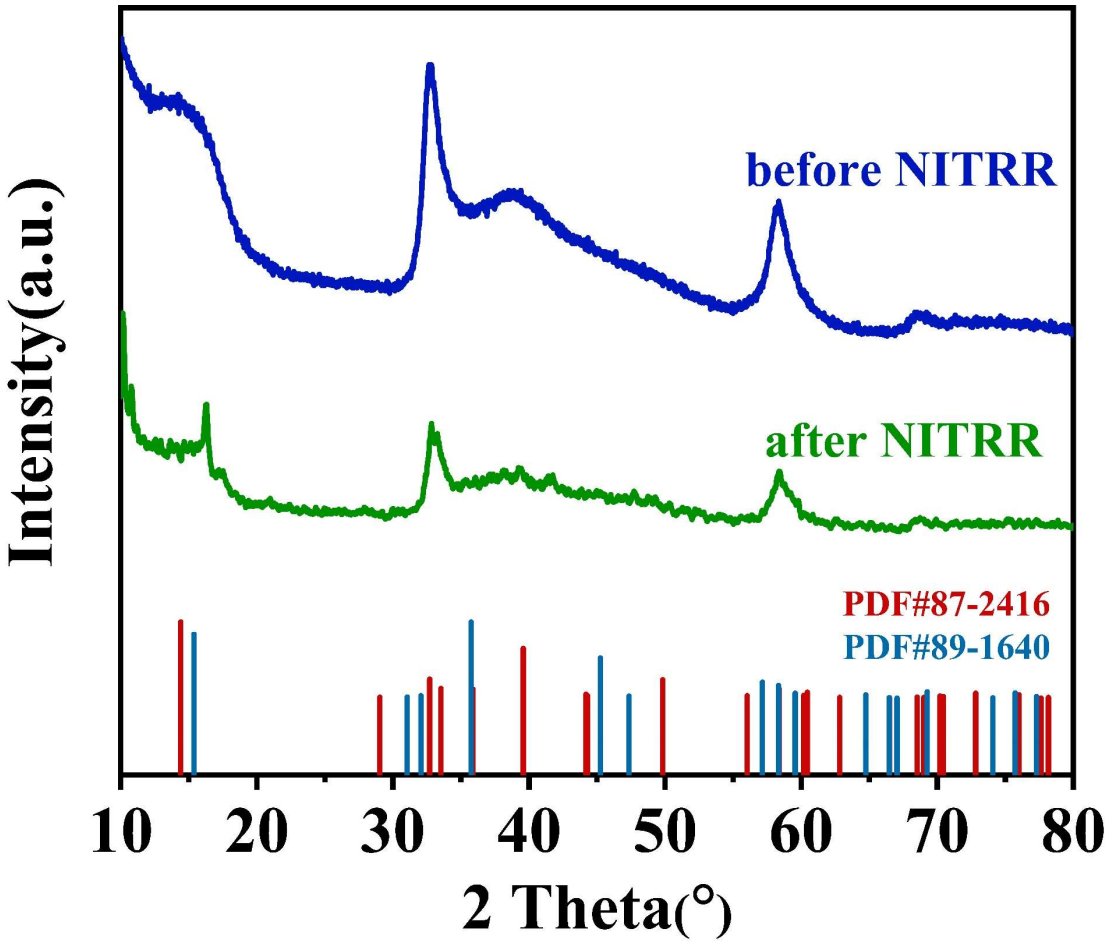

Fig. S6. XRD patterns of 15%V-MoS_2 electrocatalyst before and after electrochemical NITRR.

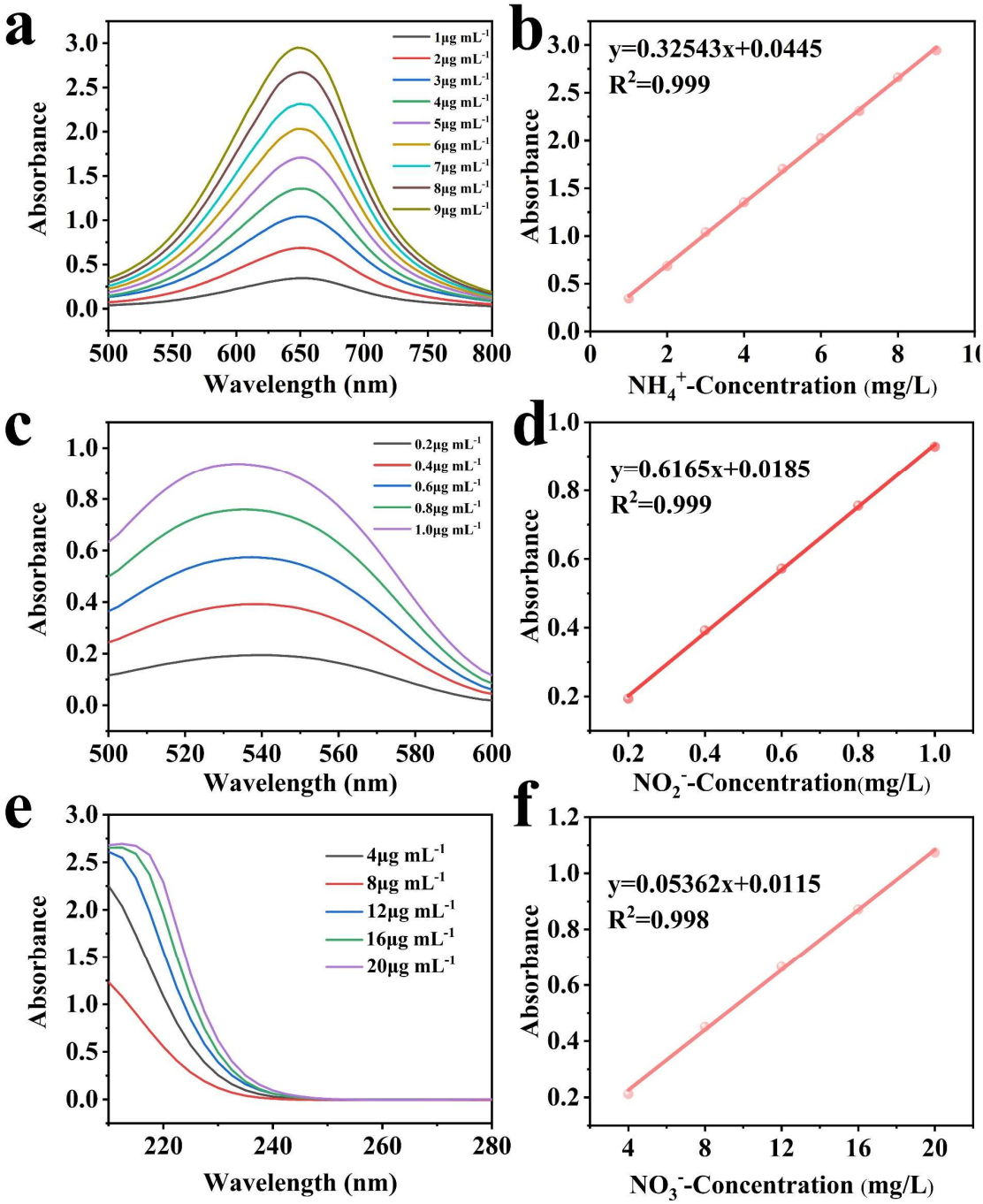

Fig. S7. (a) UV-vis absorption spectra with various NH_4^+ ions in 0.5 M Na_2SO_4 after incubation for 2 h. (b) Calibration curve used for estimation of NH_3 from the NH_4^+ ion concentration. (c) UV-vis spectra of NO_2^- solution with different concentrations after incubated for 20 min. (d) Corresponding liner fitting between absorbance and NO_2^- concentration. (e) UV-vis spectra of NO_3^- solution with different concentrations after incubated for 15 min. (f) Corresponding liner fitting between absorbance and NO_3^- concentration,

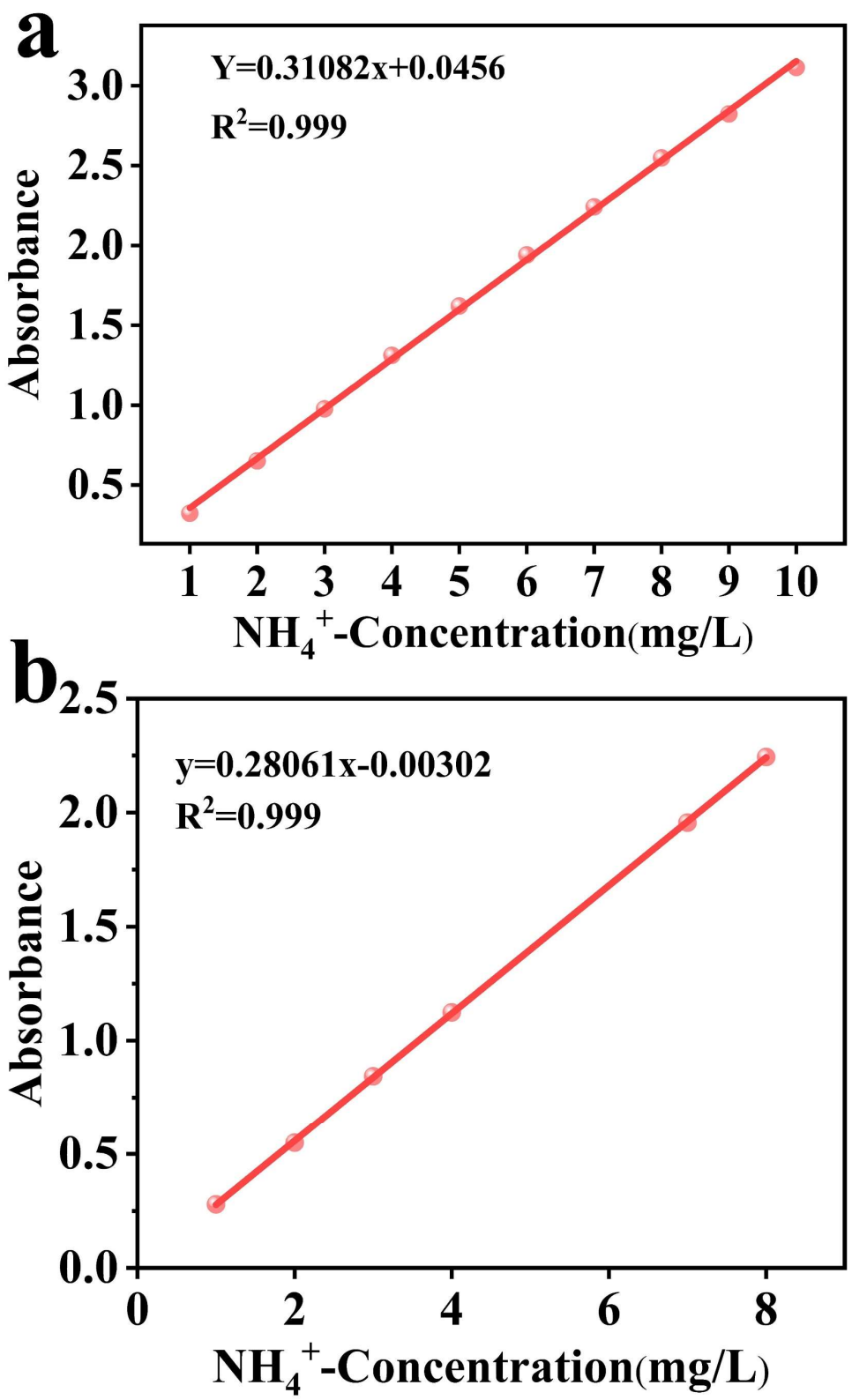

Fig. S8. Calibration curves used for estimation of NH_3 from the NH_4^+ ion concentration (a) in 0.05 M H_2SO_4 and (b) in 0.1M NaOH.

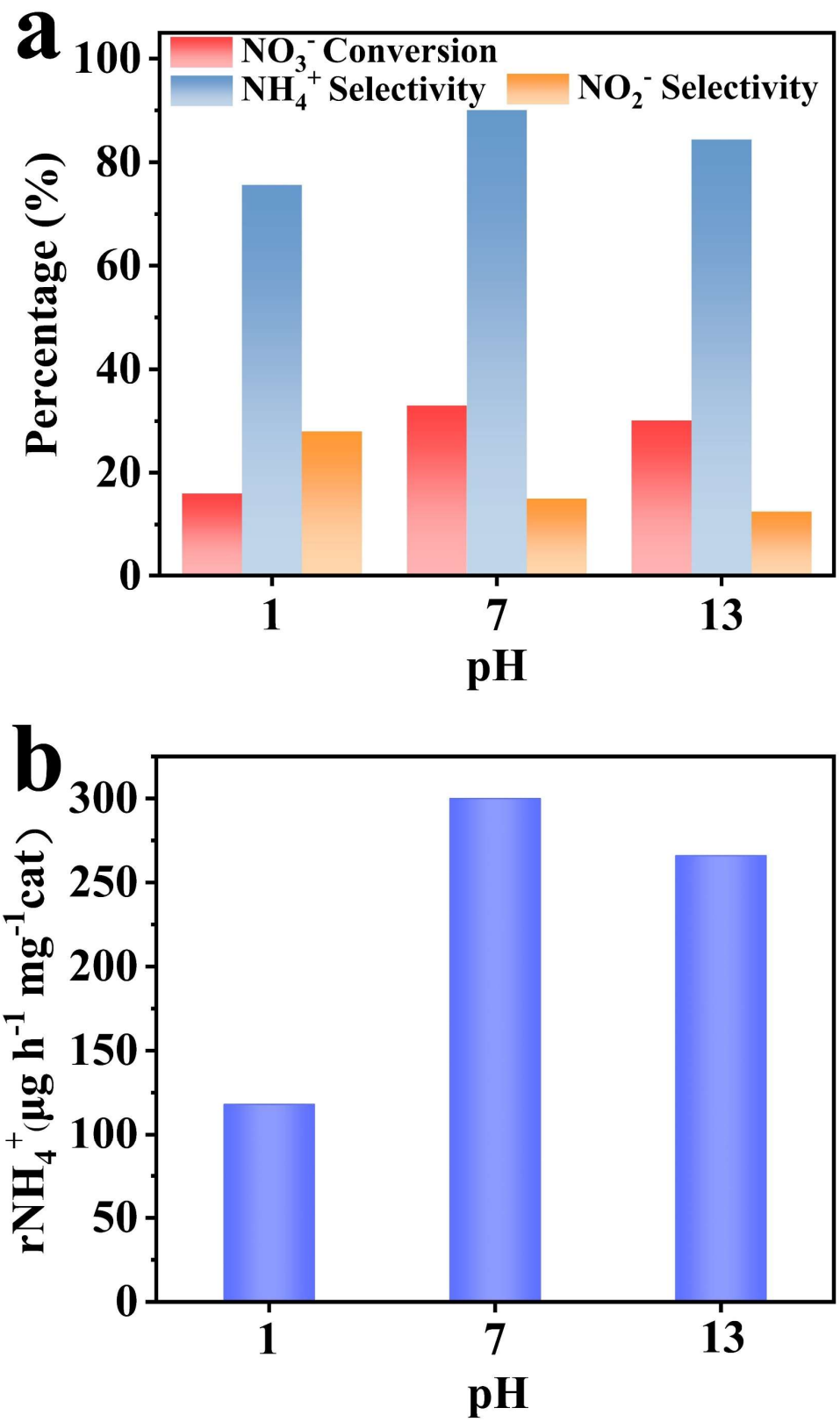

Fig. S9. NITRR electrochemical performance of 15%V-MoS_2 catalyst at pH=1, 7, 13 (a) NO_3^-–N conversion, NH_4^+–N, NO_2^-–N selectivity and (b) NH_4^+–N yield.

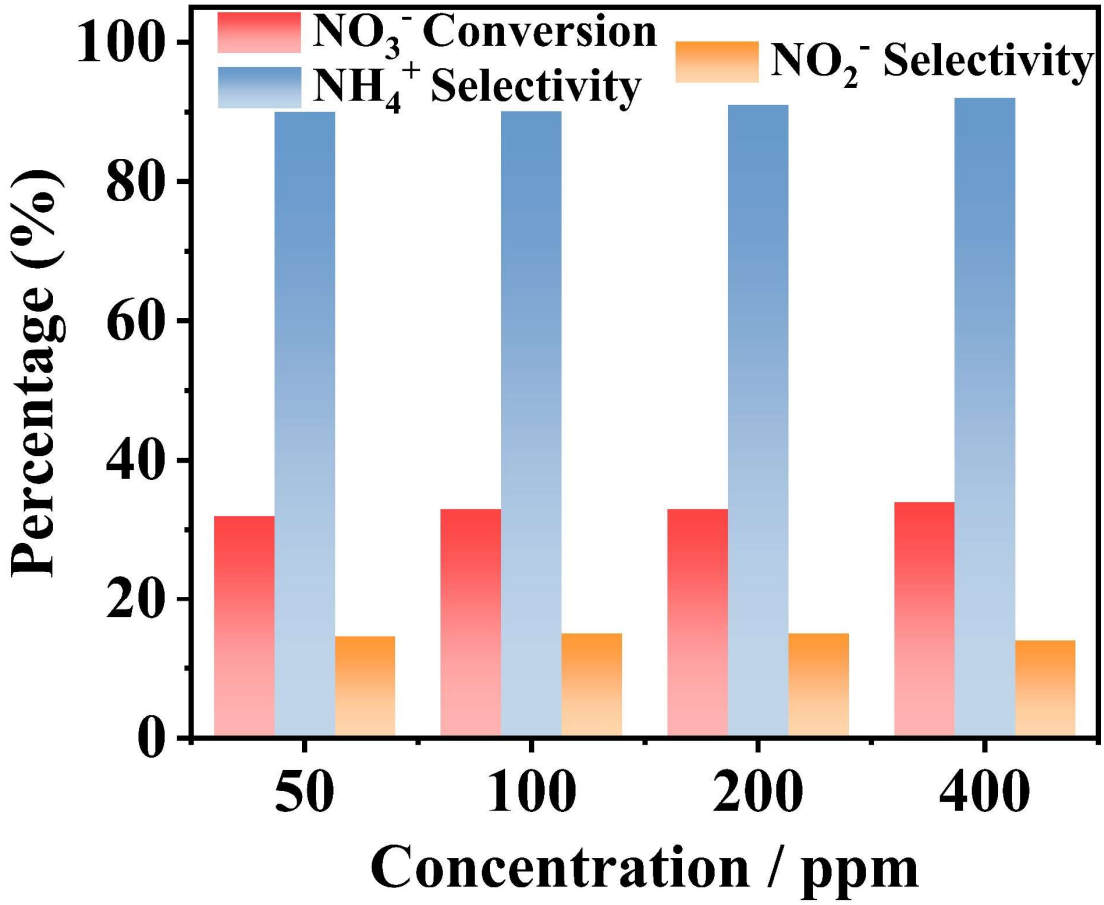

Fig. S10. NITRR behaviors of 15%V-MoS_2 catalyst at different initial nitrate concentrations.

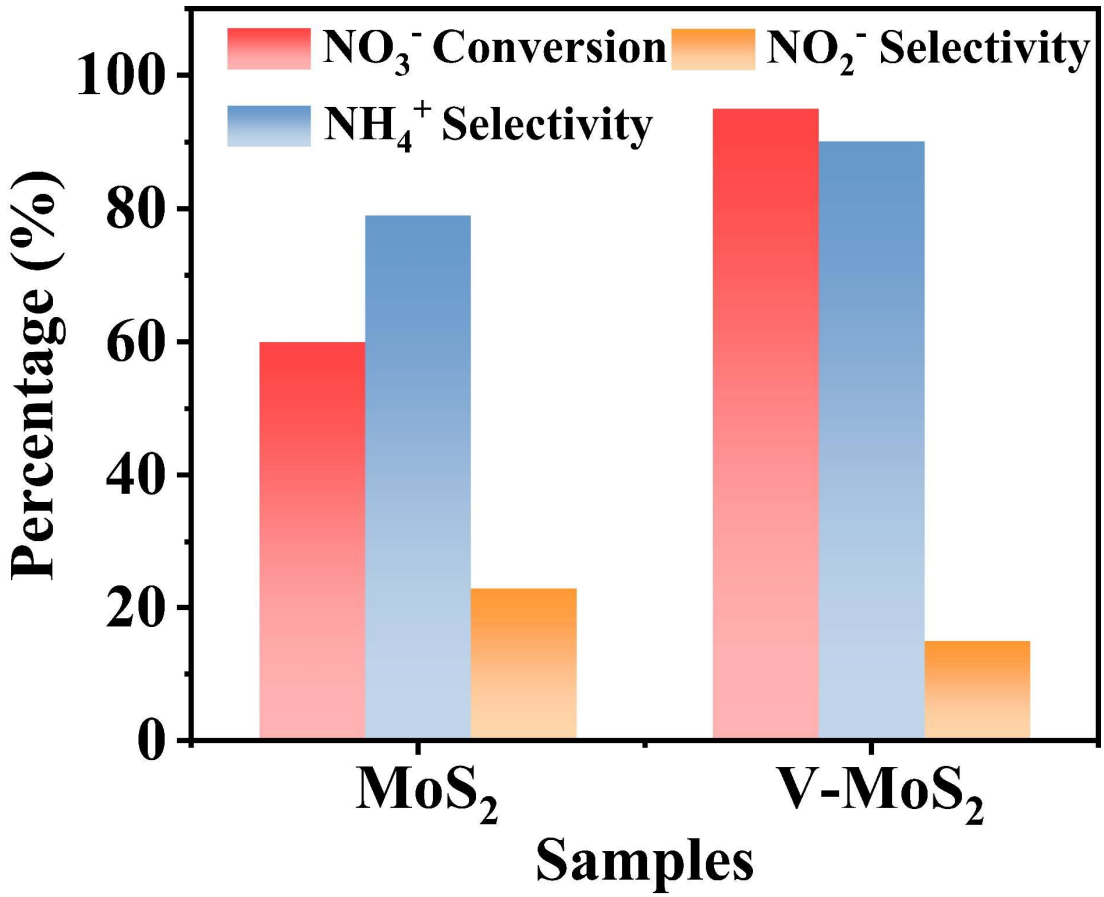

Fig. S11. NITRR behaviors of MoS_2 catalyst compared with 15%V-MoS_2.

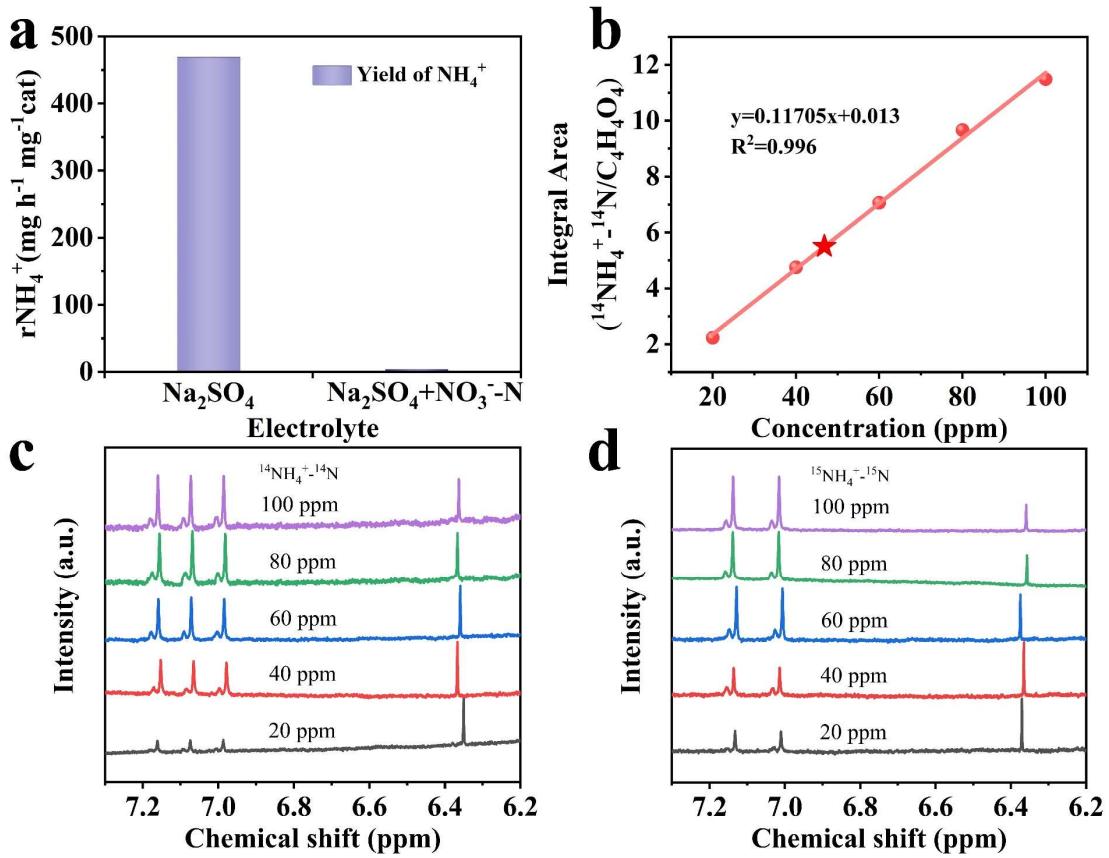

Fig. S12. (a) Ammonium yield rate over 15%V-MoS_2 in Na_2SO_4 electrolyte with and without nitrate, (b) The standard curve of integral area ($14NH_4^+$−14N/ $C_4H_4O_4$) against $14NH_4^+$−14N concentration, (c) The 1H NMR spectra (600 MHz) of $15NH_4^+$ with different $15NH_4^+$-15N concentration, (d) The 1H NMR spectra (600 MHz) of $14NH_4^+$ with different $14NH_4^+$−14N concentration.

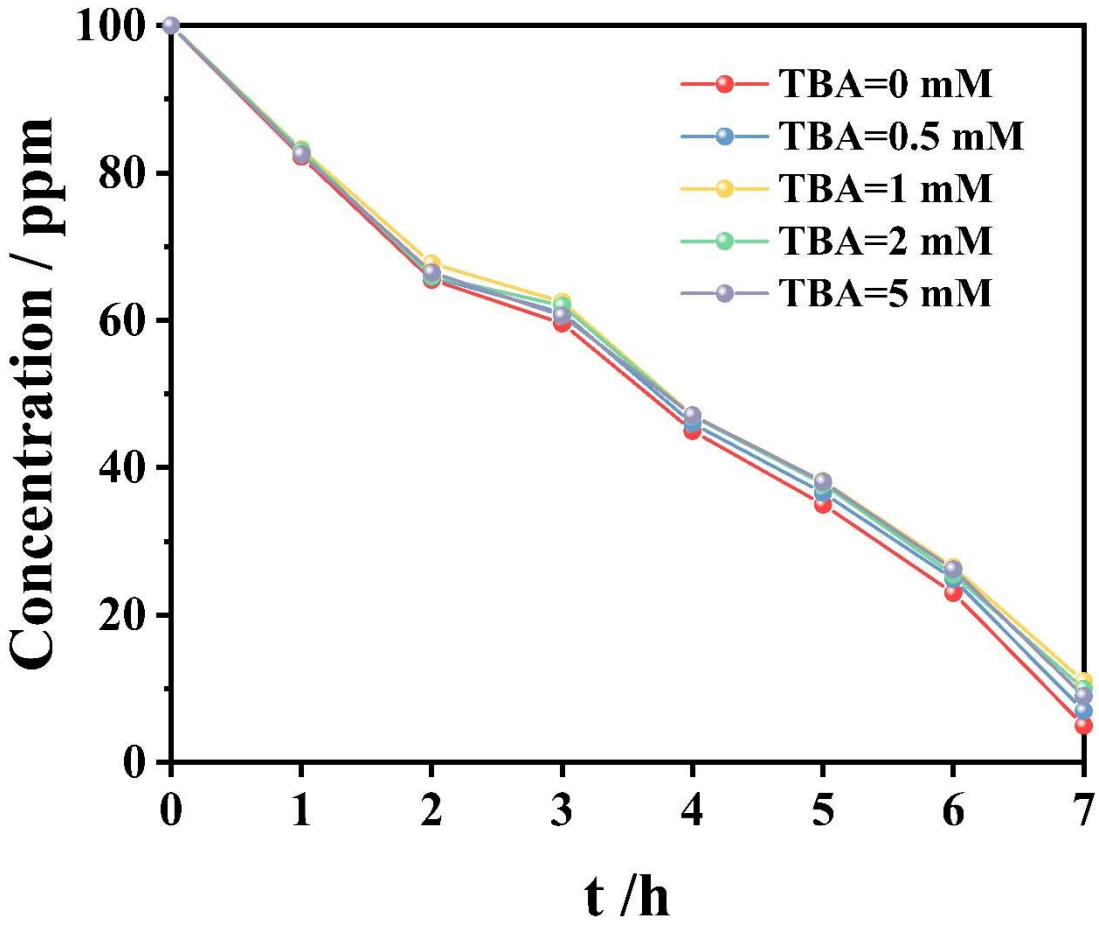

Fig. S13. Concentration decay kinetics with various TBA concentrations. Experimental conditions: an H-type electrolytic cell, 0.5M Na_2SO_4, 100 ppm NO_3^- solution (70 mL), −1.1V (vs. RHE).

Table S2. Comparison of the electrochemical NITRR activity for 15%V-MoS_2 with that of other NITRR catalysts under ambient conditions.

Catalyst	Electrolyte	Optimum potential or Current density	NO_3^- conversion	Ammonia Selectivity	Ref.
15%V-MoS_2	0.5M Na_2SO_4, 100 ppm NO_3^--N	-1.1V (vs. RHE)	33% (2h), 55% (4h), 95% (7h),	90.1% (2h), 89.1% (4h), 89.5% (7h)	**This work**
Fe@N-C	50 mM Na_2SO_4, 50 ppm NO_3^--N	-1.3 V (vs. SCE)	83% (24h), <75% (7h)	<75%	2
Cu/rGO/GP	0.02 M NaCl, 280 ppm NO_3^--N	-1.4 V (vs. SCE)	96.8% (3 h)	29.93% (3 h)	3
Co3O4/Ti mesh	0.1 M K_2SO_4, 100 g L^{-1} KNO_3	−0.65 V (vs. RHE)	_	33.6% (3 h)	4
$Pd_{0.27}Cu_{0.73}$/SS	0.1 M Na_2SO_4, 50 ppm NO_3^--N	3 mA cm^{-2}	99% (4 h)	< 25% (4 h)	5]
Sn/PdPt	0.1 M $HClO_4$, 0.01 M $NaNO_3$	-0.2 V (vs. Ag/AgCl)	59% (5 h)	13 ± 1% (5 h)	6
Cu-Sn-Bi	0.1M Na_2SO_4, 100 ppm $NaNO_3$	-1.4 V (vs. RHE)	88.43% (5 h)	17.04% (5 h)	7
Fe	0.5 g/L Na_2SO_4, 50 ppm NO_3^--N	-1.35V (vs. Ag/AgCl)	91% (4 h)	28% (4 h)	8
BDD (boron-doped diamond)	0.1g/L Na_2SO_4 50 ppm NO_3^--N	-2.0V (vs. Ag/AgCl)	42% (2 h)	8.9% (2 h)	9
Co_3O_4/Ti	0.05 mol L^{-1} Na_2SO_4, 100ppm NO_3^-	10 mA cm^{-2}	99% (3h)	70% (3h)	10]
Bi_2O_3-CC	0.5 M Na_2SO_4, 50 ppm $NaNO_3$	10 mA cm^{-2}	84.9% (3h)	80.3% (3h)	11

FeNPs@MXene	0.5 M Na_2SO_4, 100 ppm NO_3^--N	-0.95 V (vs. RHE)	97.8% (24h)	76.8% (24h)	12
Cu-Pd plate	1400 mg L^{-1} Na_2SO_4, 135.5 ppm NO_3^--N	-1.1 V (vs. RHE)	64% (6h)	35% (6h)	13
Ni-TiO_2 nanotube	0.5 g L^{-1} Na_2SO_4, 50 ppm NO_3^--N	-2.1 V (vs. RHE)	93.4% (1.5h)	53.53% (1.5h)	14
Pd–MnO_2-Ov/Ni foam	50 mM of Na_2SO_4, 90 ppm NO_3^--N	-0.85V (vs. RHE)	40% (3h)	90% (3h)	15
CuPd@DCLMCS/ CNTs	0.1 M Na_2SO_4, 100ppm NO_3^--N	-1.3V (vs. SCE)	95% (36h)	5% (36h)	16

References

1. Y. Li, Y. K. Go, H. Ooka, D. He, F. Jin, S. H. Kim and R. Nakamura, *Angew. Chem. Int. Ed. Engl.*, 2020, **59**, 9744-9750.
2. W. Duan, G. Li, Z. Lei, T. Zhu, Y. Xue, C. Wei and C. Feng, *Water Res.*, 2019, **161**, 126-135.
3. D. Yin, Y. Liu, P. Song, P. Chen, X. Liu, L. Cai and L. Zhang, *Electrochimica. Acta*, 2019, **324**, 134846.
4. Y. Wang, Y. Yu, R. Jia, C. Zhang and B. Zhang, *Natl. Sci. Rev.*, 2019, **6**, 730-738.
5. Y.-J. Shih, Z.-L. Wu, C.-Y. Lin, Y.-H. Huang and C.-P. Huang, *Appl. Catal., B*, 2020, **273**, 119053.
6. M. M. Hossain, T. Kawaguchi, K. Shimazu and K. Nakata, *J. Electroanal. Chem.*, 2020, **864**, 11404.
7. W. Gao, L. Gao, J. Meng, D. Li, Y. Guan, L. Cui, X. Shen and J. Liang, *Water Sci. Technol.*, 2019, **79**, 198-206.
8. W. Li, C. Xiao, Y. Zhao, Q. Zhao, R. Fan and J. Xue, *Catal. Lett.*, 2016, **146**, 2585-2595.
9. P. Kuang, K. Natsui and Y. Einaga, *Chemosphere*, 2018, **210**, 524-530.
10. L. Su, K. Li, H. Zhang, M. Fan, D. Ying, T. Sun, Y. Wang and J. Jia, *Water Res.*, 2017, **120**, 1-11.
11. M. Chen, J. Bi, X. Huang, T. Wang, Z. Wang and H. Hao, *Chemosphere*, 2021, **278**, 130386.
12. W.-J. Sun, L.-X. Li, H.-Y. Zhang, J.-H. He and J.-M. Lu, *ACS Sustainable Chem. Eng.*, 2022, **10**, 5958-5965.
13. T. Favarini Beltrame, M. C. Gomes, L. Marder, F. A. Marchesini, M. A. Ulla and A. Moura Bernardes, *J. Water Process Eng.*, 2020, **35**, 101189.
14. F. Liu, K. Liu, M. Li, S. Hu, J. Li, X. Lei and X. Liu, *Chemosphere*, 2019, **223**, 560-568.
15. Y. Wang, S. Shu, M. Peng, L. Hu, X. Lv, Y. Shen, H. Gong and G. Jiang, *Nanoscale*, 2021, **13**, 17504-17511.
16. H. Xu, J. Wu, W. Luo, Q. Li, W. Zhang and J. Yang, *Small*, 2020, **16**, e2001775.